arXiv:1210.1721v1 [nucl-th] 5 Oct 2012

Strictly finite range potential for light PET isotopes

P. Salamon[1], T. Vertse[1,2], and L. Balkay[3]

[1]*Institute of Nuclear Research of the Hungarian Academy of Sciences,*
Debrecen, PO Box 51, H–4001, Hungary

[2]*University of Debrecen, Faculty of Informatics,*
PO Box 12, H–4010 Debrecen, Hungary

[3]*University of Debrecen, Institute of Nuclear Medicine,*
Medical and Health Science Center,
PO Box 12, H–4010 Debrecen, Hungary

(Dated: October 8, 2012)

Abstract

By adjusting the parameters of the new phenomenological nuclear potential introduced recently by P. Salamon and T. Vertse [1] (SV) to the global potential sets of Perey and of Becchetti and Greenlees, it is shown that the SV potential well approximates the cut-off Woods–Saxon (CWS) form even if its second term is set to zero. The important difference between the CWS and SV potentials is that CWS jumps to zero at the cut-off radius, while the SV potential goes to zero smoothly. We fitted the single-term SV potential to the global potentials, and compared the spectra and the pole trajectories of neutron single-particle states generated by some light neutron-deficient nuclei that are most often used in positron emission tomography (PET): ^{13}N, ^{15}O and ^{18}F. The CWS and the SV energies agree reasonably well, and only the pole trajectories, which span extremities, are substantially different.

PACS numbers: 21.10.Pc, 25.40.Dn, 87.59.Vb

Keywords: neutron optical potential, light PET isotopes

The positron emitting nuclides used in PET are usually produced by irradiation of light targets by light charged particles accelerated by cyclotrons. The most productive reactions are $^{14}\mathrm{N}(p,\alpha)^{11}\mathrm{C}$, $^{13}\mathrm{C}(p,n)^{13}\mathrm{N}$, $^{15}\mathrm{N}(p,n)^{15}\mathrm{O}$, and $^{18}\mathrm{O}(p,n)^{18}\mathrm{F}$. In three of the four reactions listed above neutrons are emitted, so the exit channel is neutron scattering from $^{13}\mathrm{N}$, $^{15}\mathrm{O}$, and $^{18}\mathrm{F}$, respectively. Neutron scattering is generally described in the framework of the optical model, in which the mean field of the target nucleus is represented by a phenomenological optical potential.

The geometry of the optical potential terms is generally fixed and only the strengths of its terms are assumed to be energy-dependent. The optical potential is constructed almost exclusively from cut-off Woods–Saxon (CWS) terms and their derivatives. The strict finite range (SFR) is emphasized [2] since whenever the radial Schrödinger equation is solved numerically, we in fact use SFR potentials since we match the numerical solution to a linear combination of the incoming and outgoing Coulomb waves at a finite distance $r = R_{\mathrm{match}}$, and calculate the S-matrix from this matching. For neutron scattering the Coulomb waves reduce to the solutions of the Riccati–Hankel differential equation.

The CWS can be written as:

$$V^{\mathrm{CWS}}(r,R,a,R_{\max}) = -V_0 f_{\mathrm{CWS}}(r,R,a,R_{\max}) \ , \tag{1}$$

where the radial shape is

$$f_{\mathrm{CWS}}(r,R,a,R_{\max}) = \begin{cases} \frac{1}{1+e^{\frac{r-R}{a}}} & , \text{if } r \ < \ R_{\max} \\ 0 & , \text{if } r \ \geq \ R_{\max} \ . \end{cases} \tag{2}$$

Nuclear scattering may be described in terms of resonances. It was shown earlier [1] that in the CWS potential the positions of broad resonances do depend on the value of the cut-off radius $R_{\max}$ [2, 3], although it has no physical meaning. This is caused most probably by the discontinuity of the CWS form at $R_{\max}$. Therefore, the cut-off radius is an important parameter of the CWS form in Eq. (2). The two-other parameters of the CWS form are the radius R and the diffuseness a.

In Ref. [1] two of us proposed a more convenient SFR potential, the Salamon–Vertse (SV) potential instead of the CWS potential. The SV potential tends to zero smoothly, and even its derivatives become zero at and beyond a finite radial distance. Thus the SV potential has the attractive mathematical property that its derivative exists in the whole $r \in (0,\infty)$ range.

The SV potential may be specified [1] as a linear combination of the function

$$f(r,\rho) = \begin{cases} e^{\frac{r^2}{r^2-\rho^2}} & \text{, if } r \; < \; \rho \\ \;0 & \text{, if } r \; \geq \; \rho \; , \end{cases} \tag{3}$$

and its derivative with respect to r, $f'(r,\rho)$. The SV potential may thus be written [3] as a product of a potential depth V_0 and a radial shape $f_{\rm SV}(r,c,\rho_0,\rho_1)$ with three adjustable parameters ρ_0, ρ_1 and c:

$$V^{\rm SV}(r) \; = \; -V_0 f_{\rm SV}(r,c,\rho_0,\rho_1) \; , \tag{4}$$

$$f_{\rm SV}(r,c,\rho_0,\rho_1) \; = \; f(r,\rho_0) - cf'(r,\rho_1) \; . \tag{5}$$

To describe attraction, the coefficient c has to be non-negative. With the usual choice ($\rho_0 > \rho_1$), the SV form vanishes at ρ_0, i.e., $f_{\rm SV}(r \geq \rho_0, c, \rho_0, \rho_1) = 0$. The SV radial form has three parameters just like the radial form of the CWS potential.

To make the SV potential resemble the CWS shape as much as possible, we fit its three parameters to the radial form factor of the CWS shape $f_{\rm WS}$ by minimizing

$$\Delta(\rho_0,\rho_1,c) = \int_0^{\rho_0} \left[f_{\rm SV}(r,c,\rho_0,\rho_1) - f_{\rm WS}(r,R,a,R_{\rm max}) \right]^2 dr \; . \tag{6}$$

The integration in Eq. (6) can be performed by using equidistant mesh-points $r_i = ih$ over the range of the integration:

$$\Delta(\rho_0,\rho_1,c) = \sum_{i=1}^{n} \left[f_{\rm SV}(r_i,c,\rho_0,\rho_1) - f_{\rm WS}(r_i,R,a,R_{\rm max}) \right]^2 \; . \tag{7}$$

There are several families of global optical model potentials with CWS real parts. In most cases the radial shapes (the radius parameter R and diffuseness a) are fixed, and only the strengths V_0 are varied. The spin-orbit potential for a particle with a spin of $s = \frac{1}{2}\hbar$ is

$$V_{\rm so}^{\rm WS}(r,R_{\rm so},a_{\rm so},R_{\rm max}) = V_{\rm so}^{\rm WS} h_{\rm WS}(r,R_{\rm so},a_{\rm so},R_{\rm max}) \; 2(\vec{l} \cdot \vec{s}) \; , \tag{8}$$

with a radial form involving the derivative of the central potential

$$h_{\rm WS}(r,R,a,R_{\rm max}) = -\frac{1}{r} f'_{\rm WS}(r,R,a,R_{\rm max}) \; . \tag{9}$$

The radial factor of the spin-orbit term is also cut to zero at $R_{\rm max}$ (the derivative $f'_{\rm CWS}(r)$ would be infinite at $R_{\rm max}$). It is easy to define the spin-orbit potential for the SV potential since $f'_{SV}(r)$ exists everywhere:

$$V_{\rm so}^{\rm SV}(r,c,\rho_0,\rho_1) = V_{\rm so}^{\rm SV} h_{SV}(r,c,\rho_0,\rho_1) \; 2(\vec{l} \cdot \vec{s}) \; , \tag{10}$$

with

$$h_{SV}(r, c, \rho_0, \rho_1) = -\frac{1}{r} f'_{SV}(r, c, \rho_0, \rho_1) \ . \qquad (11)$$

The radii of the potential terms for a target with mass number A_T are scaled by $A_\mathrm{T}^{1/3}$, i.e., $R = r_0 A_\mathrm{T}^{1/3}$. The radii and diffuseness can be different for the different terms of the potential.

There are two classical global nucleon potential sets given by Perey [4] and by Becchetti and Greenlees [5] long ago. In a more recent study of the isospin-dependent global neutron-nucleus optical model potential [6], the old Becchetti–Greenlees potential was used as a starting point. In this work, we also use the Perey and the Becchetti–Greenlees parameters for simplicity. Since the SV potential is quite new, and its mass number dependence has not been explored [1], we fitted the SV parameters to the global potential shapes by minimizing Eq. (6) for a broad range of mass numbers. The A_T dependence of the resulting SV parameters is quite regular except in the region of the light nuclei, and the SV potentials reproduce the CWS shape quite well. The mixing coefficient c decreases with decreasing A_T as one can see in Fig. 1. To avoid the discrepancy for light nuclei, we imposed the requirement that the derivative of the SV potential should also be similar to the derivative of the CWS shape by minimizing

$$\Delta(\rho_0, \rho_1, c_1) = \sum_{i=1}^{n} \left[f_\mathrm{SV}(r_i, c_1, \rho_0, \rho_1) - f_\mathrm{WS}(r_i) \right]^2 + \lambda \left[\frac{df_\mathrm{SV}(r_i, c_1, \rho_0, \rho_1)}{dr} - \frac{df_\mathrm{WS}(r_i)}{dr} \right]^2 . \qquad (12)$$

With a value of $\lambda = 25$ fm^2, the resulting SV potential became reasonably smooth and similar to the CWS shape that we wanted to approximate.

With the Perey [4] parameters for the central potential ($r_0 = 1.25$ fm and $a = 0.65$ fm) we obtain that the best-fit SV parameters are $\rho_0 = 1.85 A_\mathrm{T}^{1/3}$ fm, $\rho_0 - \rho_1 = 3.2a$ fm (a the diffuseness), $c = -0.03 + 0.004 A_\mathrm{T}$. With the Becchetti–Greenlees [5] geometry ($r_0 = 1.17$ fm and $a = 0.75$ fm), the radius of the central potential is, of course, somewhat smaller, but the best-fit SV parameters behave similarly to the case of Perey's potential. With A_T decreased, the mixing parameter c decreased for both global potentials as one can see in Fig. 1. The second term is apparently needed to produce the nearly constant inner section of the potential, and since the inner part of a light nucleus is very small, the second term has no significance for them. For example, the SV parameters conforming the Perey geometry are $\rho_0 = 5.084$ fm, $\rho_1 = 3.244$ fm and $c = 0.040$, while those reproducing the Becchetti–Greenlees shape are $\rho_0 = 4.957$ fm, $\rho_1 = 2.728$ fm and $c = 0.011$. Thus, for the light nuclei under consideration, it is reasonable to take simply $c = 0$.

TABLE I: Geometrical parameters of the SV and CWS potentials for ^{13}N, ^{15}O and ^{18}F nuclei. All distances are in fm units.

A_{T}	ρ_0	R	a
^{13}N	4.79	2.94	0.65
^{15}O	5.01	3.08	0.65
^{18}F	5.3	3.28	0.65

In Fig. 2, the CWS shape and its derivative with the SV potential and its derivative ($c = 0$) are compared for the Perey geometry applied to the ^{18}F target. The CWS parameters are listed in Table I. This shape is described best by a $c = 0$ SV form with a range $\rho_0 = 5.3$ fm. The SV shape is similar to the CWS shape although now we have a single parameter to adjust. The best-fit value of ρ is shifted a bit from the optimal value of ρ_0 found with two terms (from $\rho_0 = 4.975$ fm to $\rho = 5.3$ fm). The difference between the CSW and the SV potentials grows with the distance, as the SV shape goes to zero much faster than the CWS shape.

It is interesting to see how these differences influence the single-particle energies in the two potentials. In Table II we show the neutron single-particle energies ϵ_{nlj} calculated in the nucleus ^{19}F with CWS potential parameters $V_0^{\mathrm{WS}} = 60$ MeV, $r_0 = 1.25$ fm, $a = 0.65$ fm, $V_{\mathrm{so}}^{\mathrm{WS}} = 7$ MeV and with the fitted SV potential. The spin-orbit potential terms were calculated according to Eqs. (8) and (10), respectively. The strength of the SV potential has been readjusted so as to reproduce the 1s energy obtained with the CWS shape, which resulted in $V_0 = 59.934$ MeV. In Fig. 2 one can observe that the difference between the original Perey form and the adjusted SV form is magnified in the derivatives, which are used in the spin-orbit potentials $h_{\mathrm{WS}}(r)$ and $h_{\mathrm{SV}}(r)$. The spin-orbit strength for CWS potential was $V_{\mathrm{so}} = 7$ MeV. This value caused a gap of 1.93 MeV between the 0p orbits and a gap of 3.2 MeV between the 0d orbits. With a $V_{\mathrm{so}}^{\mathrm{SV}} = 30$ MeV, we were able to produce roughly the same gaps (1.97 MeV for $l = 1$ and 3.28 MeV for $l = 2$).

We obtained similar agreements for the two other nuclei, ^{15}O and ^{13}N. Table III represents the calculated single-particle energies for ^{13}N.

We can conclude that for light nuclei the $c = 0$ version of the SV potential is a good approximant to the phenomenological CWS potential, since it produces almost the same

TABLE II: Neutron single-particle energies (in MeV) in the CWS and the SV potentials outside the ^{18}F core.

n, l, j	Energy (CWS)	Energy (SV)
$0s_{1/2}$	-38.926	-38.119
$0p_{3/2}$	-23.998	-23.610
$0p_{1/2}$	-22.0674	-21.640
$1s_{1/2}$	-7.697	-7.697
$0d_{5/2}$	-8.985	-9.048
$0d_{3/2}$	-5.779	-5.769

TABLE III: Neutron single-particle energies (in MeV) in the CWS and the SV potentials outside the ^{13}N core.

n, l, j	Energy (CWS)	Energy (SV)
$0s_{1/2}$	-35.045	-36.746
$0p_{3/2}$	-18.620	-20.368
$0p_{1/2}$	-16.318	-17.958
$1s_{1/2}$	-3.400	-3.400
$0d_{5/2}$	-3.067	-4.247
$0d_{3/2}$	-0.003	-0.548

spectrum as the CWS potential.

To see whether the SV potential is a good substitute for the CWS form, one has to compare their performances for positive energies as well. It is, however, difficult to compare continuum entities. What we do instead is a comparison in terms of S-matrix poles, whereby we can also check whether the features of the CWS potential observed [2] for heavy nuclei are present for light nuclei as well. It has been found in Ref. [2] that the real parts of the starting points of the s-wave pole trajectories follow Newton's rule: $R\text{Re}(k_n) \approx n\pi$ [7]. Here R denotes the range of the potential beyond which it is zero. In the CWS potential, R is the cutoff radius R_{max}. The $\text{Re}(k_n)$ values calculated for the CWS potential follow this rule approximately if n is not very small.

The high-precision numerical solution of the radial equation was performed by using Ixaru's method [8]. In Fig. 3 the pole trajectories are shown for ^{18}F in a CWS potential well with $R_{\rm max} = 15$ fm. By fitting the calculated Re(k_n) values for $n < 5$ with a first-order polynomial, we can deduce $R = 14.8$ fm. This agrees reasonably well with the $R_{\rm max} = 15$ fm value used.

In Fig. 4 we show the calculated Re(k_n) values for the corresponding SV potential. If Newton's rule were valid, the trajectories would start from the vicinity of these lines. The starting points, however, overshoot the trajectories. Thus the SV trajectories satisfy the rule less accurately. From the starting points of $n > 3$ we obtain $R = 4.84$ fm for the slope. The deviation from the $\rho_0 = 5.3$ fm value is not negligible and even a bit larger than the deviation found in Ref. [2]. It is more important that the pole trajectories produced by the SV potential behave quite regularly in contrast to the CWS potential in which the $n = 1$ trajectory shows a strange circulating path. Similar strange behavior was also found for ^{208}Pb [9] and was attributed to the sharp cut-off of the CWS potential.

The substantial differences between the pole trajectories may cause some concern as to the performance of the SV potential in scattering calculations, but the trajectories span a broad range of potential depths, which extend to physically irrelevant regions. From the point of view of scattering calculations in the region of isotope production, the most relevant property of the potentials is their low-energy behavior near the threshold. By putting some of the states at the threshold, we could also show that depths of the Perey and the SV potentials are almost the same, which demonstrates that the two potentials must behave very similarly for low-energy scattering relevant to the production of PET isotopes.

This work was supported by the ENIAC CSI Project (No.120209).

---

[1] P. Salamon and T. Vertse, Phys. Rev. C **77**, 037302 (2008).

[2] J. Darai, A. Rácz, P. Salamon, and R. G. Lovas, Phys. Rev. C **86**, 014314 (2012).

[3] A. Rácz, P. Salamon, and T. Vertse, Phys. Rev. C **84**, 037602 (2011).

[4] F. G. Perey, Phys. Rev. **131**, 745 (1963).

[5] F. D. Becchetti and G. W. Greenlees, Phys. Rev. **182**, 745 (1969).

[6] Xiao-Hua Li, Lie-Wen Chen, Nucl. Phys. **A874**, 62 (2012).

[7] R. G. Newton, Scattering Theory of Waves and Particles, Springer Verl., New York Inc., 1982.

[8] L. Gr. Ixaru, Numerical Methods for Differential Equations and Applications, D. Reidel, Publ. Comp., Dordrecht/Boston/Lancaster, 1984.

[9] T. Vertse, R. G. Lovas, P. Salamon, and A. Rácz, talk on the Int. Conf. Nuclear Structure and Dynamics II, held in Opatija, Croatia, July 13-19, 2012, the Proceedings will be published by the AIP later.

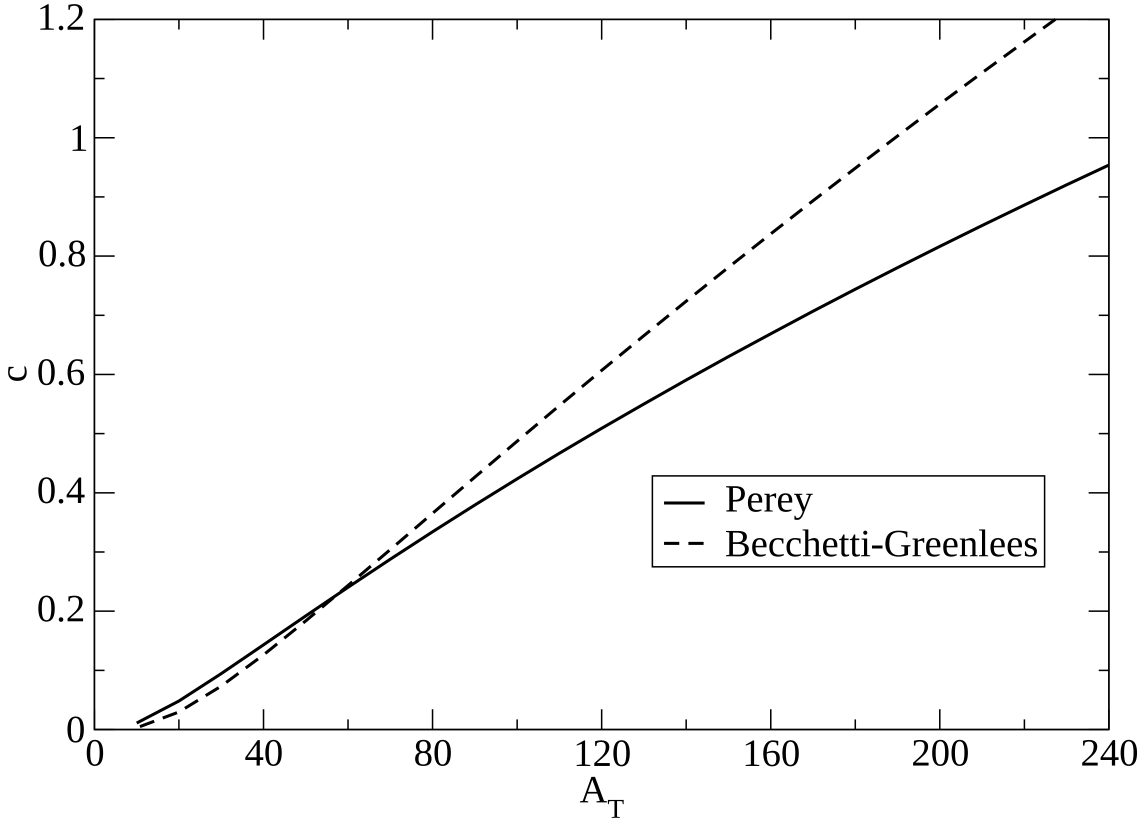

FIG. 1: Dependence of the mixing coefficient c on the target mass-number A_{T}.

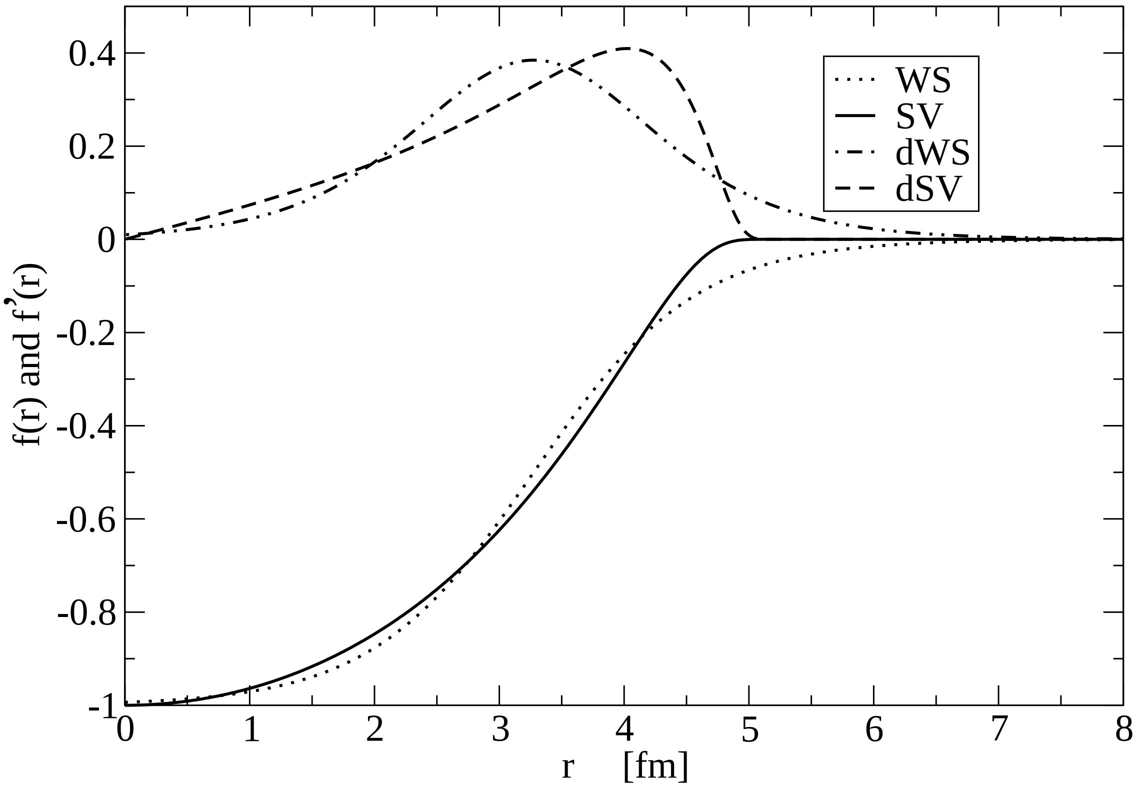

FIG. 2: Radial shapes of the CWS and SV ($c = 0$) potentials and its derivatives for ^{18}F.

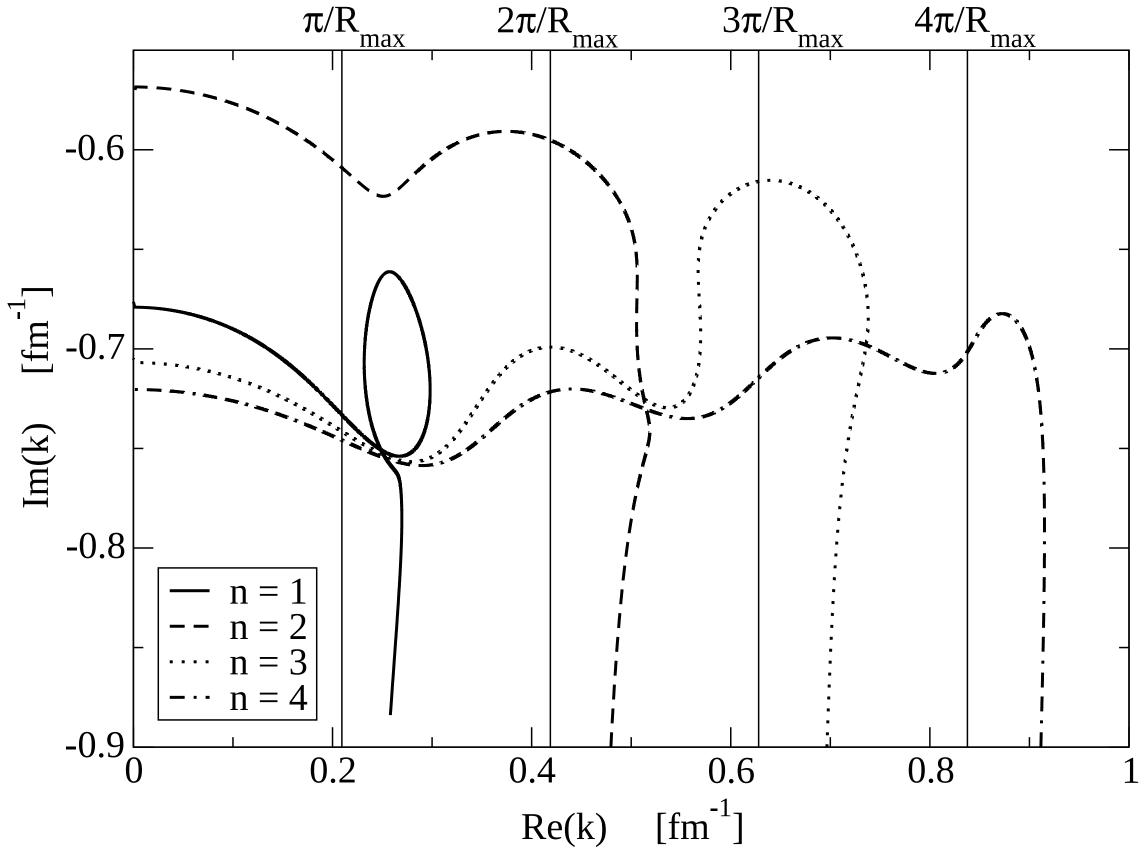

FIG. 3: Trajectories of the poles of the S-matrix in $l = 0$ partial wave in the CWS potential of Perey's shape. The vertical lines show the $\mathrm{Re}(k) = \frac{n\pi}{R_{\max}}$ values.

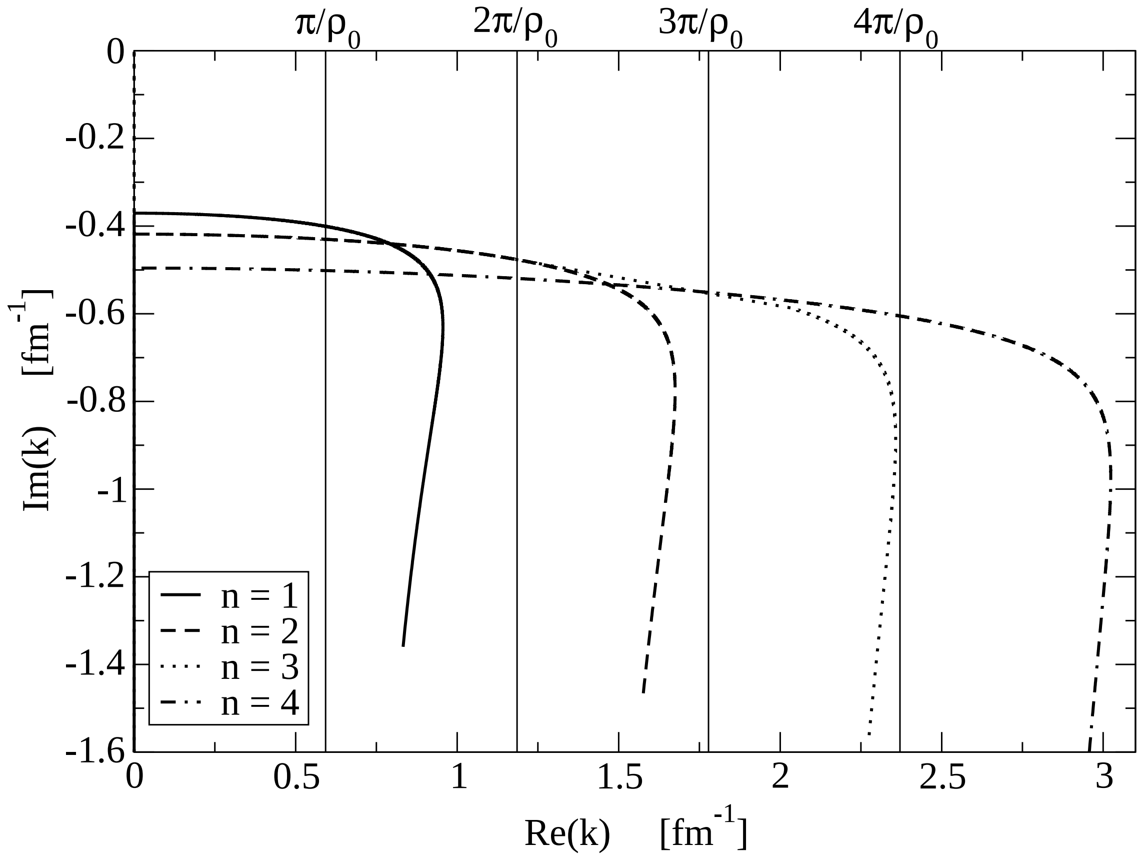

FIG. 4: Trajectories of the poles of the S-matrix in $l = 0$ partial wave in the SV potential of Perey's shape. The vertical lines show the $\text{Re}(k) = \frac{n\pi}{\rho_0}$ values.